[13] Rossettos, J. N. and Parisse, R. F., "The Dynamic Response of Cylindrical and Conical Shells," *Journal of Applied Mechanics*, Vol. 36, No. 2, Feb. 1969, p. 271.

[14] Budiansky, B. and Roth, R. S., "Axisymmetric Dynamic Buckling of Clamped Shallow Spherical Shells," TN D-1510, 1962, NASA, p. 597.

[15] Mescall, J., "Large Deflections of Spherical Shells under Concentrated, Distributed and Ring Loadings," *Proceedings of Fourth Southwestern Conference on Applied Mechanics*, Pergamon Press, New York, 1968.

[16] Evenson, H. A. and Evan-Iwanowaski, R. M., "Dynamic Response and Stability of Shallow Spherical Shells Subject to Time-Dependent Loading," *AIAA Journal*, Vol. 5, No. 5, May 1967, p. 969.

JULY 1971 AIAA JOURNAL VOL. 9, NO. 7

Large Strain, Elasto-Plastic Finite Element Analysis

LAWRENCE D. HOFMEISTER,* GILBERT A. GREENBAUM,† and DAVID A. EVENSEN‡
TRW Systems Group, Redondo Beach, Calif.

A method is presented for the large strain, elasto-plastic analysis of two-dimensional structures by the finite element method. An incremental variational principle is used to develop the finite element equilibrium equations for use in a piecewise linear solution procedure. The present formulation differs from other papers in that the variational principle leads to a set of equations which include an equilibrium check. The equilibrium check can be employed at any point in the incremental solution process, with a Newton-Raphson iteration, to reduce any cummulative error in nodal point equilibrium. Such errors are caused by linearizing the displacement equilibrium equations, and can build up to such an extent that the computed results are meaningless. The equilibrium check and corrective cycling procedure presented herein prevent the computed load-deflection behavior from straying from the true equilibrium path, and they represent a major contribution of this paper.

Nomenclature

A	=	cross-sectional area of truss member
a_s, a_o	=	initial and final inner radius, respectively, of folded sheet
C_{ijkl}	=	constitutive operator
E, E_p	=	elastic and postyield modulii, respectively
ΔE_{ij}	=	incremental Green's strain tensor
$\{E\}$	=	vector of residual error forces
e	=	strain at inner radius of folded sheet
$\{\Delta F\}$	=	vector of incremental forces
Δf_i	=	component of element force vector
k_{ij}	=	elements of incremental stiffness matrix
$k_{ij}^{(G)}$	=	elements of geometric stiffness matrix
$[K]_N$	=	system stiffness matrix at step N
$[K^{(G)}]_N$	=	system geometric stiffness matrix at step N
L	=	length of truss member
N	=	load step N
q	=	applied pressure load
$\{\Delta R\}$	=	incremental system displacements
Δr_i	=	incremental elemental displacement
s	=	surface
t	=	thickness of bent sheet
$\Delta T_i, T_i, T_i^{(0)}$	=	incremental, total and initial surface tractions, respectively
Δu_i	=	incremental displacement
v	=	volume
X_i	=	local (initial) coordinates
x_i	=	current coordinates
δ_{ij}	=	Kronecker delta
$\delta(\ )$	=	variational operator
ϵ	=	error measure
ϵ_i	=	error force at element coordinate i
$\Delta\epsilon_{ij}$	=	linear portion of strains
$\Delta\eta_{ij}$	=	nonlinear strains
ϕ_{ij}	=	shape functions
$\Delta\sigma_{ij}, \sigma_{ij}, \sigma_{ij}^{(0)}$	=	incremental, total and initial stress tensors
σ_y	=	yield stress
μ	=	Poisson's ratio
$\Delta\omega_{ij}$	=	incremental rotation tensor

Presented at the AIAA/ASME 11th Structures, Structural Dynamics, and Materials Conference, Denver, Colo., April 22-24, 1970; submitted July 9, 1970; revision received December 3, 1970. This work was supported by NASA-JPL under Contract NAS 7-682.

* Member of the Technical Staff, Structures Department, Mechanical Engineering Laboratory.

† Section Head, Advanced Technology Department, Applied Mechanics Laboratory; now with Universal Analytics, Inc., Los Angeles, Calif. Member AIAA.

‡ Member of the Technical Staff, R & A Staff, Mechanical Engineering Laboratory.

Introduction

MANY authors have applied the finite element method to geometrically nonlinear problems.[1-8] From this work, basically three classes of finite element formulations can be defined: Class 1) incremental methods without equilibrium checks; Class II) direct solutions of the governing nonlinear equations; and Class III) incremental methods with equilibrium checks.

Historically, Class I was the first finite element approach to solving geometrically nonlinear problems.[1,8-10] In this method, the load is applied to the structure in small increments, and the incremental displacements due to each load step are determined. Incremental stresses and strains are computed at each step and used in the following load step. Although this method is computationally very fast, it has the disadvantage that equilibrium at any particular load level is not necessarily satisfied. No attempt is made to determine if equilibrium requirements are indeed met, and the same problem must be repeatedly solved using successively smaller load steps to assess the solution accuracy.

The direct solution method (Class II) involves applying the total load to the structure and computing the total response by using mathematical iterative techniques. This approach may be subdivided into two distinct categories; a) direct minimization of the potential energy, and b) direct solution of the nonlinear algebraic equilibrium equations.

Mallett and Schmit[5,11] employ mathematical programing methods to numerically minimize the potential energy functional. An advantage of this method is that minimum computer storage is required since no system stiffness matrices are assembled; rather, the potential energy for the system is obtained simply as the scalar sum of the energies of the individual elements. However, if second-order gradient methods are used to perform the energy search, in order to speed convergence, this advantage disappears. Additionally, only stable equilibrium configurations can be determined, making the interpretation of the results awkward in some cases.

In the second category mentioned under Class II, mathematical iterative methods are applied to the governing nonlinear equilibrium equations. Oden[6] has applied this scheme successfully to nonlinear elasticity problems. Newton-Raphson iteration was used to solve the equilibrium equations.

A major disadvantage of both Class II methods is that they are not applicable to path dependent problems, such as plastic deformation. A summary of the Class I and II methods is given by Mallett and Marcal.[2]

The third class of solution techniques involves determining the incremental solutions due to a series of load steps and applying equilibrium checks and (if necessary) corrections, to the solution. Unlike Class I, this method insures that the solution satisfies equilibrium throughout the loading history.[3,4,12] This procedure was introduced by Wissmann.[12] There are numerous computational schemes that are associated with this class. For example, in order to minimize computer time, Brebbia and Connor[3] correct for equilibrium at only every four steps. Murray and Wilson[4] iterate at every load step to satisfy equilibrium, but do not necessarily use the "exact" incremental stiffness matrix. Wissman[12] uses a "progressive iteration with back-substitution" method for each load step. The present paper uses the Class III method with two different computational refinements. The first is to iterate at each load level, using the exact stiffness matrix, until equilibrium is satisfied. The second technique is similar to the Class I approach but attempts to correct for equilibrium at each load step by using the unbalance force from one step as a pseudo load in the next step. This method is computationally equivalent to Class I but has the advantage that the solution is continuously monitored and improved.

Other types of nonlinear problems which have been solved using the finite element procedure deal with material nonlinearities, in particular elastoplastic behavior. Two general methods have been developed for the elastoplastic analysis of structures. These are a) the initial strain method, and b) the tangent modulus method.

The initial strain method[13,14] treats the plastic strains at each incremental load step as initial strains for the next load step. In this method, plasticity effects are taken into account as pseudo loads, and the elastic stiffness matrix is used throughout the entire loading process. The advantage of this method is that for small displacement problems, the governing stiffness matrix need be built and "inverted" only once.

The tangent modulus method,[7,15–18] on the other hand, is based upon the incremental stress-plastic strain laws of plasticity. In this method, plasticity effects are accounted for in the stiffness matrix, which is updated at each load step. It should be noted that when solving large deflection problems by the incremental methods (Classes I and III), a new stiffness matrix is required at each load step. Thus, the large deflection incremental methods combine well with the tangent modulus method, since it also requires a new stiffness matrix at each load step. As pointed out by Marcal,[19] the tangent modulus method offers the additional advantage that larger load increments can be used than in the initial strain method.

Only a few references have been found in which both geometric nonlinearities and plasticity are treated within the framework of finite element theory.[7,18,20] Both Felippa[7] and Marcal[18] use a Class I method with the tangent modulus approach, while Armem and Pifko uses a Class I method with the initial strain approach.[20]

The present paper develops the governing incremental finite element equations for large strain, elasto-plastic problems. The formulation presented is similar to that given by Felippa[7] but uses a different variational principle. Felippa's derivation is based on an incremental variational principle that assumes the stresses at the reference state are in equilibrium with the applied loads. This leads to an incremental finite element formulation which does not check to determine if equilibrium is satisfied (i.e., Class I method). The present paper does not assume a priori that the reference state is in equilibrium. Consequently, the variational principle used herein leads to a Class III formulation, and equilibrium is checked and controlled throughout the loading history.

Analytical Formulation

In this section, the general formulation of the piecewise linear incremental solution of structures problems, involving both material and geometric nonlinearities, will be presented. This formulation is based on an incremental variational principle as given by Washizu.[21]

Incremental Variational Principle

The present paper uses an incremental formulation for the large strain, elasto-plastic problem. In the incremental variational principle presented by Washizu, the body is considered at an arbitrary reference state of the load path. It is assumed that all state variables are known at the reference state. The reference state may be regarded as the initial stressed state for determining the stresses, strains and displacements of the current state. The current state is assumed to be incrementally close to the reference state. The local initial coordinate system X_i for an element in the body is taken as a Lagrangian frame for the current state.

This coordinate system is assumed to be inscribed on the body, and when the body deforms in going from the reference configuration to the current configuration these coordinates also become deformed. A global reference system is used to assemble all such elements of the body which, for convenience, coincides with the local coordinate system X_i.

Let Δu_i (measured along the X_i coordinate direction) be the incremental deflections of a point in the body in going from the reference to the current state. Then

$$x_i = X_i + \Delta u_i \tag{1}$$

describes the relationship between the local coordinates (current coordinates) and the initial coordinates.

Consider a structure at the beginning of a particular loading increment N. At this time, the initial coordinates X_i and current coordinates x_i are identical. Assume that stresses $\sigma_{ij}^{(0)}$ and surface tractions $T_i^{(0)}$ are acting on the structure at this time, i.e., prior to the addition of the increment of load for step N. These stresses and loads are with respect to the initial coordinate axis and are referred to a unit of area before the addition of the load increment. The stresses are therefore "true" stresses. For future reference, the area and volume of an element before the load increment is applied will be referred to as the "undeformed" area and volume, respectively. The area and volume after the load increment is applied will be referred to as the "deformed" area and volume, respectively. Next, impose on the structure the incremental surface tractions ΔT_i. These give rise to additional stresses $\Delta\sigma_{ij}$ incremental displacements Δu_i, and distort the coordinates x_i. Thus the total stresses and surface tractions at the end of load increment N are given by

$$\sigma_{ij} = \sigma_{ij}^{(0)} + \Delta\sigma_{ij} \tag{2}$$

$$T_i = T_i^{(0)} + \Delta T_i \tag{3}$$

The stress tensor σ_{ij} is referred to a unit of area before the addition of the incremental loads for step N (undeformed area), but is with respect to the current axes x_i.[22] Likewise, T_i is referred to the undeformed area and current axes.

The principle of virtual work[21] for incremental load step N is, neglecting body forces

$$\int_v(\sigma_{ij}^{(0)} + \Delta\sigma_{ij})\delta(\Delta E_{ij})dV = \int_s(T_i^{(0)} + \Delta T_i)\delta(\Delta u_i)dS \quad (4)$$

where ΔE_{ij} is the incremental Green's strain tensor, and all integrals are referred to the undeformed volume of the element. The strain tensor can be written as

$$\Delta E_{ij} = \Delta\epsilon_{ij} + \Delta\eta_{ij} \quad (5)$$

where $\Delta\epsilon_{ij}$ will lead to linear strain-displacement relations, and $\Delta\eta_{ij}$ to nonlinear expressions. The incremental constitutive law in Lagrangian variables is[22]

$$\Delta\sigma_{ij} = C_{ijkl}\Delta E_{kl} \quad (6)$$

where C_{ijkl} may include the effect of past loading. For example, Marcal[18] gives a convenient form for the constitutive law for elastoplastic problems which was used for the work reported herein. Using Eqs. (2) and (3) in Eq. (4), and neglecting higher order products of incremental strains gives

$$\int_v[\sigma_{ij}^{(0)}\delta(\Delta\eta_{ij}) + \Delta\epsilon_{kl}C_{ijkl}\delta(\Delta\epsilon_{ij})]dV = \int_s\Delta T_i\delta(\Delta u_i)dS - [\int_v\sigma_{ij}^{(0)}\delta(\Delta\epsilon_{ij})dV - \int_s T_i^{(0)}\delta(\Delta u_1)dS] \quad (7)$$

If it is now assumed that the initial stress state, denoted by $\sigma_{ij}^{(0)}$ and $T_i^{(0)}$, is in equilibrium prior to the addition of the incremental loads for step N, then the last two integrals in Eq. (7) vanish, and a formulation similar to that of Felippa[7] or Murray and Wilson[4] results. However, due to the numerical incremental solution technique for solving a large strain problem, the initial stress state may *not* be in equilibrium before load step N. As will be shown in a later section, it is possible to derive an equilibrium error check if these terms are retained.

Note that the total stresses σ_{ij} resulting from load step N become initial stresses for step $(N + 1)$. For step N, these stresses are referred to a unit of undeformed area, and current axes x_i. However, for step $(N + 1)$, these stresses must be referred to deformed area and the initial axes X_i. The relation between the stress tensor σ_{ij} and the initial stress tensor $\sigma_{ij}^{(0)}$ is[22]

$$\sigma_{ij}^{(0)} = |\partial x/\partial X|^{-1}\sigma_{kl}(\partial x_i/\partial X_k)(\partial x_j/\partial X_l) \quad (8)$$

where $|\partial x/\partial X|$ is the determinant of the matrix $[\partial x_i/\partial X_j]$. From Eq. (1)

$$\partial x_i/\partial X_k = \delta_{ik} + \Delta u_{i,k} \quad (9)$$

gives the derivatives of Eq. (8), and

$$|\partial x/\partial X|^{-1} \simeq (1 - \Delta u_{1,1} - \Delta u_{2,2} - \Delta u_{3,3}) \quad (10)$$

the scaling factor. A similar transformation holds for surface tractions.

For plane stress and plane strain analysis, the strain-displacement relations are

$$\Delta\epsilon_{ij} = \tfrac{1}{2}(\Delta u_{i,j} + \Delta u_{j,i}) \quad (11)$$

$$\Delta\eta_{ij} = \tfrac{1}{2}\Delta u_{k,i}\Delta u_{k,j} \quad (12)$$

and will be used to complete the virtual work principle. However, other nonlinear strain-displacement equations, such as those for finite plate displacement theory, could be used. Substituting Eqs. (11) and (12) in Eq. (7) gives the final form of the incremental virtual work statement as

$$\int_v(\sigma_{ij}^{(0)}\Delta u_{k,i}\delta\Delta u_{k,j} + C_{ijkl}\Delta u_{k,l}\delta\Delta u_{i,j})dV = \int_s\Delta T_i\delta\Delta u_i dS - (\int_v\sigma_{ij}^{(0)}\delta\Delta u_{i,j}dV - \int_s T_i^{(0)}\delta\Delta u_i dS) \quad (13)$$

The stress transformation, Eq. (8) becomes

$$\sigma_{ij}^{(0)} = (1 - \Delta\epsilon_{kk})\sigma_{ij} + (\Delta\epsilon_{jk} + \Delta\omega_{jk})\sigma_{ik} + (\Delta\epsilon_{ik} + \Delta\omega_{ik})\sigma_{jk} \quad (14)$$

where the incremental rotation is

$$\Delta\omega_{ij} = \tfrac{1}{2}(\Delta u_{i,j} - \Delta u_{j,i}) \quad (15)$$

Finite Element Formulation

To derive the discrete element form of Eq. (13), the incremental displacements within each element are approximated by

$$\Delta u_k = \phi_{ik}\Delta r_i \quad (16)$$

where the ϕ_{ik} are interpolating[7] or shape functions, and the Δr_i are incremental nodal point displacements. The interpolating functions should satisfy certain requirements if the numerical solution is to represent an upper bound to the true solution. Substituting Eq. (16) into Eq. (13) leads to

$$(k_{ij}^{(G)} + k_{ij})\Delta r_j = \Delta f_i + \epsilon_i \quad (17)$$

for each element where

$$k_{ij}^{(G)} = \int_v\phi_{in,k}\sigma_{kl}^{(0)}\phi_{jn,l}dV \quad (18)$$

$$k_{ij} = \int_v\phi_{ik,l}C_{klmn}\phi_{jm,n}dV \quad (19)$$

$$\Delta f_i = \int_s\Delta T_k\phi_{ik}dS \quad (20)$$

$$\epsilon_i = \int_s T_k^{(0)}\phi_{ik}dS - \int_v\sigma_{kl}^{(0)}\phi_{ik,l}dV \quad (21)$$

The terms given in Eq. (18) form the incremental geometric, or initial stress, stiffness matrix, and the terms of Eq. (19) give the conventional incremental stiffness matrix. The incremental loading vector, for surface tractions only, is composed of the terms of Eq. (20). The components of Eq. (21) are referred to herein as *residuals*, since they can be used to measure the residual error in nodal point equilibrium at any load step.

Once an element type and shape functions have been chosen, and a material law considered, the integrals of Eqs. (18) to (21) can be evaluated, usually in closed form. Then Eq. (17) becomes

$$([k^{(G)}] + [k])_N\{\Delta r\}_N = \{\Delta f\}_N + \{\epsilon\}_N \quad (22)$$

for load step N. If the finite element shape changes during the incremental loading process prior to step N, then some approximations are introduced in the integrations for step N. This is the case for large strain problems in which so-called refined elements are used, as in the work reported herein. However, if the element size is kept small in the regions of high strain, the linearizing approximation introduced should be accurate.

Next, Eq. (22) can be evaluated for each discrete element, and by considering inter-element compatibility and boundary conditions, these can be assembled into a system of linear incremental equilibrium equations for the entire structure,

$$([K^{(G)}] + [K])_N\{\Delta R\}_N = \{\Delta F\}_N + \{E\}_N \quad (23)$$

For load step N, these equations can be easily solved for $\{\Delta R\}_N$, the nodal point displacements.

Solution Procedure

The linear incremental solution technique for nonlinear structural response problems proceeds as follows. For the first step, the terms of Eq. (23) are

$$\{E\}_1 = \{0\}$$

and since there are no initial stresses,

$$[K^{(G)}]_1 = [0]$$

Then the linear problem

$$[K]_1\{\Delta R\}_1 = \{\Delta F\}_1$$

is solved. After this first step, and after each succeeding step, nodal point coordinates are updated, and total displacements, strains and stresses are computed by adding all incremental contributions. The total stresses at the end of step N, σ_{ij}, must be transformed to $\sigma_{ij}^{(0)}$, initial stresses for step $(N+1)$, by using the transformation of Eq. (14). Note that in this type of procedure, the stiffness matrices $[K^{(G)}]_N$ and $[K]_N$ are recomputed for each load step, as indicated by the subscript N. This is due to the fact that both stresses (which effect the geometric stiffness matrix) and the stress-strain law (which effects the conventional stiffness matrix) change during the incremental solution process. For loadings which "follow" the structure, such as normal pressures, the load vector must also be updated for each step.

The step-by-step procedure is shown graphically in Fig. 1, in which R is some measure of deflection, and F a measure of applied force. Initially, ΔF_1 is applied to the structure, with $E_1 = 0$ (no initial unbalance), and the response $R_1 = \Delta R_1$ computed from Eq. (23). Note that, in general, $R_1 \neq R_1^{(T)}$, where the superscript "T" denotes true solution. Next, the residual E_2, i.e., the error associated with the first incremental step, is computed, after updating displacements, strains and stresses. This quantity can be used to check the accuracy of the incremental procedure, since it represents the unbalance in nodal point equilibrium introduced by the linearizing assumptions in the present theory. For the second incremental step, the load $(\Delta F_2 + E_2)$ is applied, giving eventually R_2. The process is continued in this manner until the error is as small as desired.

It is important to note how this method differs from the incremental procedures outlined by other investigators. First, an equilibrium check is automatically provided in the form of the residual vector $\{E\}_N$. Below it is shown how this quantity can additionally be used to reduce the equilibrium unbalance. Also, the addition of the residual vector to the force vector leads to displacements which are closer to the true values than would be obtained by using only the incremental force vector. This can be seen from the example of Fig. 1. If just ΔF_2 is added to the structure for step 2, instead of $(\Delta F_2 + E_2)$, then $\tilde{R}$ would result, which is a poorer approximation to the true displacement than R_2. Therefore, the omission of the residual vector leads to a load-deflection curve considerably above the true curve, for structures which "soften" with increasing load.

If the structural response is highly nonlinear, even the aforementioned procedure will lead to computed results

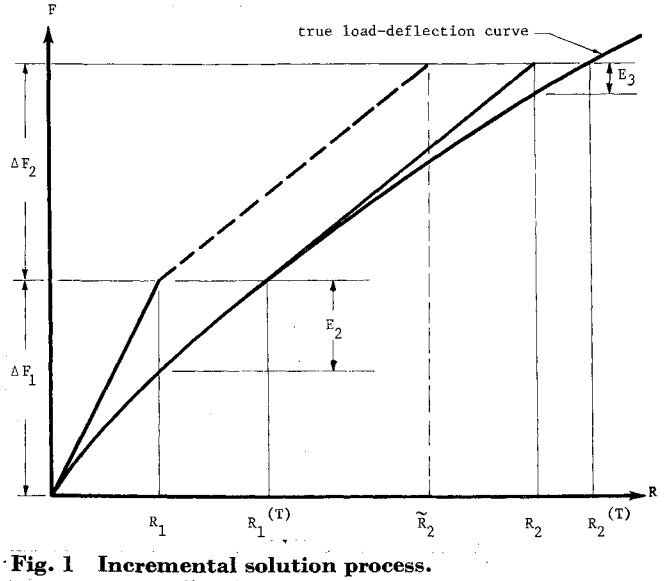

Fig. 1 Incremental solution process.

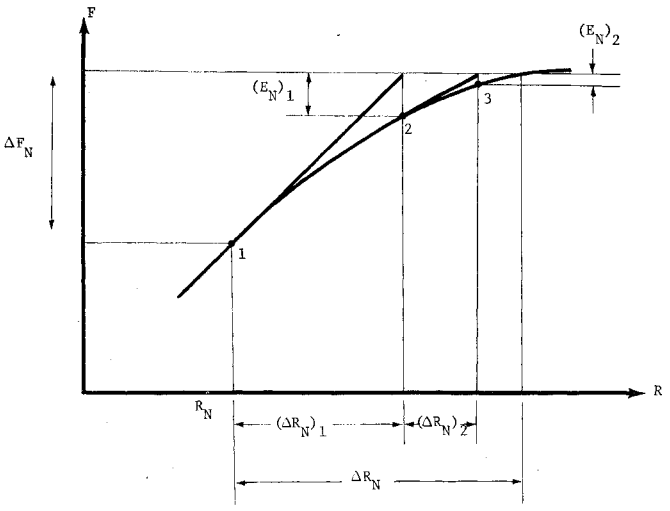

Fig. 2 Corrective iteration.

which are in error. For these types of problems, a Newton-Raphson iteration, which uses the residual vector, can be employed to reduce the error in nodal point equilibrium to any desired degree. The procedure is as follows. After $\{R\}_N$, $\{E\}_N$, etc., have been computed for step N, all information is updated. Then Eq. (23) is reassembled and resolved using only $\{E\}_N$ as a load vector. The resulting additional incremental deflections, strains and stresses are added to the previous values for step N. A new residual is computed, and the process is repeated. In fact, this iteration can be performed at constant load as often as desired. In the work reported herein, the ratio of the norms of the residual vector and total force vector

$$\epsilon = (\{E\}^T\{E\}/\{R\}^T\{R\})^{1/2}$$

is used to control the iteration by specifying that the corrective cycling continue until ϵ is less than some small number. Note that this process is similar to a Newton-Raphson iteration, as can be seen from Fig. 2. In this figure, the stiffness matrix computed for point 1 is used to predict $(\Delta R_N)_1$ as the response to ΔF_N, as a first approximation to the displacement ΔR_N. Next, the stiffness matrix for point 2 and the load of $(E_N)_1$ are used to compute $(\Delta R_N)_2$, giving $[(\Delta R_N)_1 + (\Delta R_N)_2]$ as the new approximation to ΔR_N. Note that $(E_N)_2$ is much smaller than $(E_N)_1$, indicating the iteration is converging. After suitable accuracy has been achieved, the next load increment may be added to the structure. This procedure of iteration to insure equilibrium is similar in spirit to the work of Murray and Wilson,[4] but differs basically in the way the unbalance forces are computed.

Numerical Examples

Two classes of example problems are considered herein to demonstrate the salient features of the theory. A simple single-degree-of-freedom truss problem is used to compare the various solution procedures just outlined. Several plane strain examples are also presented which display various types and degrees of nonlinear behavior.

The derivation of the elemental characteristics for the truss element is based upon a linear interpolation for displacements. The plane strain solutions were generated using the six nodal point triangular finite element introduced by Felippa.[7] In this element, a linear variation in both strains and material properties is assumed, leading to a quadratic stress variation.

The elasto-plastic constitutive relations proposed by Marcal[18] are used for the two-dimensional problems presented in the following sections. Work hardening is assumed to depend upon only the total plastic work dissipated during deformation, and thus a material can be completely charac-

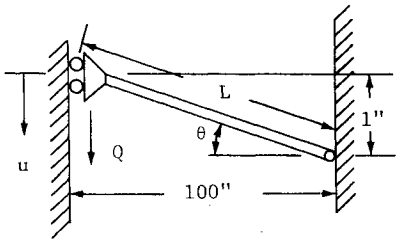

Fig. 3 Truss example problem.

terized by its uniaxial elastic modulus E, Poisson's ratio μ, yield stress σ_y, and postyield modulus E_p.

Truss Problem

The truss problem shown in Fig. 3 has been solved by several investigators.[12] The member length is L, elastic modulus E = 10,000,000 psi, and constant cross-sectional area A = 1 in.^{2} Euler buckling and bending deformation are suppressed in the analysis, and only elastic behavior is considered.

Table 1 shows three different incremental solutions to the truss example problem. The first solution is a simple linear incremental approach. As can be seen from the last column, for this case the residual error grows larger with each additional increment. For the second case, the residual has been added to the next applied load increment, resulting in much smaller errors. The final case shows the effect of only one cycle of iteration after each load step.

Hollow Cylinder

To investigate the application of the theory presented herein to elasto-plastic problems, a long cylinder subjected to internal pressure was studied. This example was used by Ref. 17 in a finite element solution. The cylinder had the characteristics given in Table 2.

A cross section cut through the cylinder was assumed to be in a state of plane strain. One-quarter of this slice was modeled using 24 linear strain triangular elements. A total load of 15 ksi internal pressure was applied in five equal increments, and the iterative correction continued until $\epsilon \leq 0.01$, after each load step.

Some typical results are shown in Figs. 4a and 4b, in which r is the radius of the cylinder. The circles represent finite element results, whereas the solid lines are from Ref. 17 using the Von Mises yield criterion and the Prandtl-Reuss flow law. Figure 4a is a normalized load-deflection curve, where $u(b)$ is the radial displacement measured at $r = b$, the outer radius of the cylinder. In this problem, the nonlinearity is caused by yielding which begins in the finite element model at the inner surface $r = a$ at a load slightly greater than P = 9 ksi (P/K = 0.78). Figure 4b is plotted for the maximum load of P = 15 ksi (P/K = 1.3). These results show that accurate solutions for displacements and stresses can be obtained using the theory proposed herein. Note also that this problem represents the most severe type of elasto-plastic behavior, since no strain hardening is assumed.

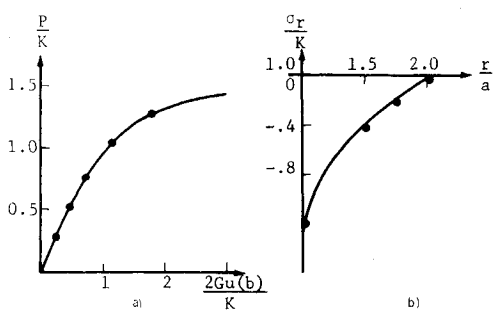

Fig. 4 a) Load vs deflection for cylinder; b) radial stress for cylinder.

Table 1 Truss problem results

Case	Load, lb	Displacement u, in.	Residual, lb
Linear incremental solution	0.5	0.0500	0.0369
	1.0	0.1086	0.0848
	1.5	0.1809	0.1527
Incremental solution with residual added to applied force	0.5	0.0500	0.0369
	1.0	0.1129	0.0551
	1.5	0.1945	0.0859
Incremental solution with one cycle of iteration after each step	0.5	0.0543	0.0003
	1.0	0.1210	0.0007
	1.5	0.2129	0.0030

Notched Tensile Specimen

A notched tensile specimen assumed to be in the condition of plane strain was analyzed in Ref. 17. However, in Ref. 17 constant strain triangular finite elements were used, whereas the present theory has been implemented using linear strain triangles. This problem is used to investigate the various solution procedures previously outlined, as was the truss problem presented earlier. The nonlinearity in this problem is caused by localized yielding of the notched sheet.

Figure 5 shows the tensile strip and the finite element mesh. Because of symmetry, only one quarter of the strip was considered. A total tension load σ = 30 ksi applied in eight equal increments.

Figure 6 shows some of the results obtained for this problem, in the form of a plot of maximum strain the x direction versus applied load. The solid dots represent a solution for which iteration at constant load was performed until $\epsilon \leq 10^{-4}$. The circles give the results obtained by adding the residual error to the incremental load for the next step. The x data points show the conventional linear incremental solution. As in the case of the truss problem, both of the methods for correcting equilibrium unbalance gave solutions significantly different from those obtained by the conventional step-by-step procedure. For this problem, the addition of the residual to the next step ("o" in Fig. 6) improved the strain predictions considerably over the conventional solutions ("x" in Fig. 6), at no additional cost in computer time.

Elastic Cylindrical Bending Problem

In Ref. 4, large deflection-moderate strain plate problems were solved by using triangular plate bending discrete elements. These solutions were limited to the elastic range and compared very well with analytical solutions given by Ref. 23. In particular, cylindrical bending of infinitely long plates due to uniform pressure was considered. This same type of plate problem was used herein to verify the theory and solution method of this paper for large deflection problems.

The infinite length plate was considered as a plane strain problem. Figure 7 shows the geometry of the plate section and the finite element grid. The width of the plate was taken as 20 in., and only half of the plate was modeled due to symmetry about the centerline. The material properties were E = 30,000 ksi and μ = 0.3, and a total load of q = 5 ksi was applied in 40 equal increments. The iteration at constant load was applied after each increment until $\epsilon \leq 10^{-4}$.

Table 2 Properties for solid cylinder

Shear modulus	G = 3,850 ksi
Inner radius	a = 1.0 in.
Outer radius	b = 2.0 in.
Elastic modulus	E = 10,000 ksi
Poisson's ratio	μ = 0.3
Yield stress in tension	σ_y = 20 ksi
Post yield modulus	E_p = 0
Yield stress in shear	σ_s = 11.54 ksi

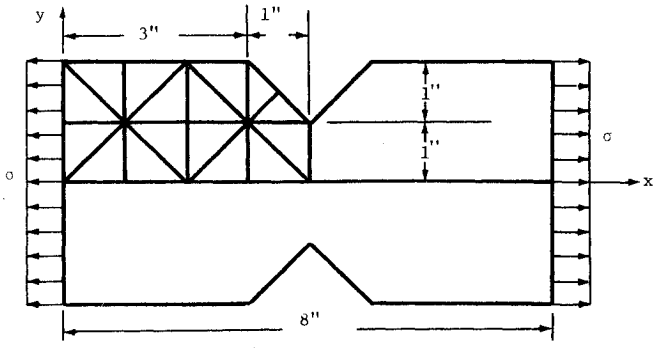

Fig. 5 Tensile strip problem.

Some of the computer results are shown in Fig. 8a and 8b as circles, with the analytical solutions from Ref. 23 represented by the solid lines. As can be seen from Fig. 8a, excellent agreement was obtained between the analytical and finite element solutions for deflection at the center of the plate. Good agreement was also obtained for membrane stresses, as measured at the center of the plate and shown in Fig. 8b.

This plate problem also demonstrated the need to use the nonlinear strain-displacement equations to compute elemental strains, and eventually stresses. In Ref. 7, only the linear portion of the strain-displacement equations was used, since in any one step, the incremental strains should be small enough that the nonlinear terms can be neglected. However, for the plate problem previously considered, large midplane strains develop mostly due to the rotation of this plane, and enters into the problem only through the nonlinear portion of the strain-displacement relations. Numerical results generated by neglecting the nonlinear contribution to the strain, even for small load increments, (0 to 2.5 ksi and 20 steps), are considerably in error. This error was eliminated by rerunning the same problem in 200 steps, at the expense of much more computer time.

Elasto-Plastic Cylindrical Bending Problem

The elastic large deflection plate cylindrical bending problem considered above was rerun using $E_p = 75$ ksi and $\sigma_y = 110$ ksi. These values were obtained by fitting a bilinear approximation to a typical true stress-true strain curve of a low-alloy structural steel. True strains greater than 20% were neglected in the fitting.

A total load of $q = 1.25$ ksi was applied to the plate in ten equal increments, and iteration after each increment was performed until $\epsilon \leq 10^{-4}$. Figure 8a and 8b show some of the numerical results for this problem. The aforementioned elastic solution is also given for comparison in these plots. From both figures it can be seen that considerable difference exists between the elastic and elastoplastic solutions for both deflections and stresses. In fact, due to the progressive yielding through the plate thickness, the slope of the load-deflection curve, Fig. 8a, changes noticeably at a load near 625 psi. Large strains were not developed during the solution to this problem.

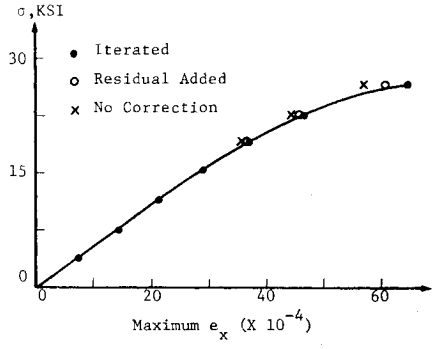

Fig. 6 Stress vs maximum strain for tensile strip.

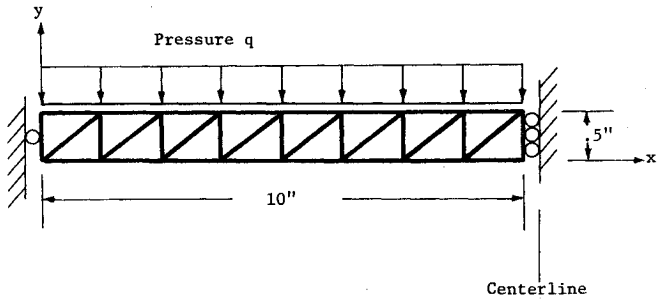

Fig. 7 Plate bending problem.

Large Strain Problem-Sheet Bending

Solutions to large deflection, elasto-plastic problems are not plentiful in the literature. However, Ref. 24 presents a problem, under the general theory of sheet bending, which can be used as a partial check on the accuracy of the theory presented herein. The problem is that of plastic bending of a wide sheet by couples applied along opposite edges. By assuming; 1) plane sections remain plane, 2) elastic deformation can be neglected, 3) the material is perfectly plastic, and 4) the Tresca yield criterion, the analysis of Ref. 24 gives the following expression for hoop strain at the inner radius:

$$e = \ln[a_o(a_s + t/2)/a_s(a_o + t/2)] \qquad (24)$$

where t is the sheet thickness, a_s the starting inner radius and a_o the final inner radius. This equation was plotted for $t = 0.02$ in. and a range of a_o values in Fig. 9 as a solid line. The starting inner radius a_s was computed from theory of elasticity as the radius at which yielding first occurs. For this problem $a_s = 14.95$ in.

A finite element model was devised to represent a portion of the sheet. The model was "loaded" by specifying displacements along one boundary such that this edge remains plane and the nodal points do not move radially along this boundary

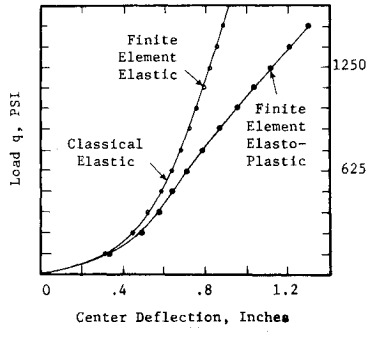

Fig. 8a Load vs deflection for plate.

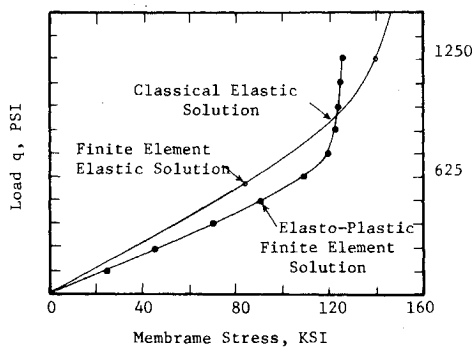

Fig. 8b Membrane stress vs load for plate.

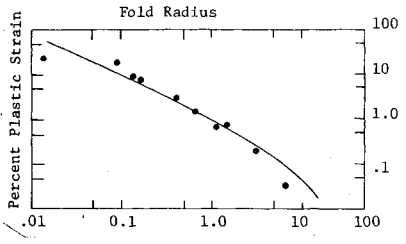

Fig. 9 Plastic strain vs fold radius for sheet bending; fold radius measured in inches.

with respect to each other. This was done to simulate the "planes remain plane" assumption in the analytical solution. The inner radius was computed by fitting a second order curve to the two nodal points on the inner surface closest to the center-line of the fold. Zero hardening was postulated to duplicate the assumptions made in the analytical model. The other input quantities were $E = 10{,}000$ ksi, $\mu = 0.33$, $\sigma_y = 6$ ksi, and $\epsilon \leq 10^{-2}$. The model was loaded, starting from a radius of $a_s = 18.30$ in. (at which the first yield occurred) to an inner radius of $a_o = 0.0125$ in. in thirteen steps. Some typical plastic hoop strains obtained for this solution are shown as dots in Fig. 9.

As can be seen from Fig. 9, the finite element solution agrees well with the analytical results over a wide range of folding radii. However, for small and large folding radii, the solutions did not agree closely. At large radii, part of the cross section of the finite element model was still elastic, whereas the analytic solution neglects elastic behavior. At small radii, shear strains grew large in the numerical model, distorting originally plane sections (except at the end boundaries). The closed-form solution assumed planes remain plane. The shear strains tended to relieve the hoop strains in the finite element idealization at small radii. Note that this problem is an example of elasto-plastic, large strain (on order of 30%), in large deflection (on order of thickness) behavior.

Conclusions

An incremental method for the prediction of elasto-plastic, large strain and deflection response of structures by the finite element method has been presented. Two different methods for the control of residual error have been discussed. It was also pointed out that the complete nonlinear strain-displacement equations must be used to compute strains.

Several plane strain example problems were solved to demonstrate the theory. All solutions were obtained using a CDC 6500 computer. Running times for the examples given herein are shown in Table 3. From Table 3, it can be concluded that efficient solutions can be obtained using the method of this paper for reasonably sized problems.

Table 3 Solution times

Example	Degrees-of-freedom	Running time, sec
Hollow cylinder	130	69
Notched strip—no correction	98	34
Notched strip—residual added	98	34
Notched strip—iterated	98	146
Elastic cylindrical bending	51	223
Plastic cylindrical bending	51	236
Large strain bending	126	376

References

[1] Turner, M. J., Clough, R. W., Martin, H. C., and Topp, L. J., "Stiffness and Deflection Analysis of Complex Structures," *Journal of the Aeronautical Sciences*, Vol. 23, No. 9, Sept. 1956, pp. 805–825.

[2] Mallett, R. H. and Marcal, P. V., "Finite Element Analysis of Nonlinear Structures," *Journal of the Structures Division*, American Society of Civil Engineering, Vol. 94, No. ST9, Sept. 1968, pp. 2081–2105.

[3] Brebbia, C. and Connor, J., Jr., "Analysis of Geometrically Nonlinear Plates and Shells by the Finite Element Method," Feb. 1968, Dept. of Civil Engineering, M. I. T.

[4] Murray, D. V. and Wilson, E. L., "Large Deflection Plate Analysis by Finite Element," *Journal of the Engineering Mechanics Division*, American Society of Civil Engineers, Vol. 95, No. EM1, Feb. 1969, pp. 143–165.

[5] Mallett, R. H. and Schmit, L. A., "Nonlinear Structural Analysis by Energy Search," *Journal of the Structures Division*, American Society of Civil Engineers, Vol. 93, No. ST3, June 1967, pp. 221–234.

[6] Oden, J. T., "Numerical Formulation of Nonlinear Elasticity Problems," *Journal of the Structures Division*, American Society of Civil Engineers, Vol. 93, No. ST3, June 1967, pp. 235–236.

[7] Felippa, C. A., "Refined Finite Element Analysis of Linear and Nonlinear Two-Dimensional Structures," Ph.D. thesis, Oct. 1966, Univ. of California, Berkeley.

[8] Popov, E. P. and Yaghmai, S., "Linear and Nonlinear Static Analysis of Axisymmetrically Loaded Thin Shells of Revolution," *Proceedings 1st International Congress on Pressure Vessel Technology*, ASME/Royal Netherlands, Sept. 1969, pp. 237–245.

[9] Argyris, J. H., "Recent Advances in Matrix Methods of Structural Analysis," *Progress in Aeronautical Sciences*, Vol. 4, Pergamon Press, Oxford, London, 1963.

[10] Argyris, J. H., Kelsey, S., and Kamel, H., "Matrix Methods of Structural Analysis," AGARDOgraph No. 72, Pergamon Press, New York, 1964.

[11] Fox, R. L., and Stanton, E. L., "Developments in Structural Analysis by Direct Energy Minimization," *AIAA Journal*, Vol. 6, No. 6, June 1968, pp. 1036–1042.

[12] Wissman, J. W., "Nonlinear Structural Analysis: Tensor Formulation," *Proceedings of Conference on Matrix Methods in Structural Mechanics*, AFFDL-TR-66-80, Oct. 1965, pp. 679–696, Wright-Patterson Air Force Base, Ohio.

[13] Gallagher, R. H., Padlog, J., and Bijlaard, P. P., "Stress Analysis of Heated Complex Shapes," *ARS Journal*, Vol. 32, May 1962, pp. 700–707.

[14] Argyris, J. H., "Elasto-Plastic Matrix Displacement Analysis of Three-Dimensional Continua," *Journal of the Royal Aeronautical Society*, TN, Vol. 69, 1965, pp. 633–635.

[15] Swedlow, J. L. and Yang, W. H., "Stiffness Analysis of Elastic-Plastic Plates," SM 65-10, 1965, Graduate Aeronautical Lab., California Institute of Technology.

[16] Pope, G. G., "The Application of the Matrix Displacement Method in Plane Elasto-Plastic Problems," *Proceedings of Conference on Matrix Methods in Structural Mechanics*, AFFDL-TR-66-80, Oct. 1965, Wright-Patterson Air Force Base, Ohio.

[17] Marcal, P. V. and King, J. P., "Elastic-Plastic Analysis of Two-Dimensional Stress Systems by the Finite Element Method," *International Journal of Mechanical Sciences*, Vol. 9, 1967, pp. 142–155.

[18] Marcal, P. V., "Large Deflection Analysis of Elasto-Plastic Shells of Revolution," *Proceedings of the AIAA/ASMC 10th Conference*, New Orleans, La., 1969.

[19] Marcal, P. V., "A Comparative Study of Numerical Methods of Elastic-Plastic Analysis," *AIAA Journal*, Vol. 6, No. 1, Jan. 1965, pp. 157.

[20] Armen, H., Pifko, A., and Levine, H. S., "A Finite Element Method for the Plastic Bending Analysis of Structures," *Proceedings of Conference on Matrix Methods in Structural Mechanics*, AFFDL-TR-68-150, Oct. 1968, Wright-Patterson Air Force Base, pp. 1301–1339.

[21] Washizu, K., *Variational Methods in Elasticity and Plasticity*, Pergamon Press, New York, 1968.

[22] Fung, Y. C., *Foundations of Solid Mechanics*, Prentice-Hall, Englewood-Cliffs, N. J., 1965.

[23] Timoshenko, S. P. and Woinowsky-Krieger, S., *Theory of Plates and Shells*, McGraw-Hill, New York, 1959.

[24] Yeh, G. C. K., "Large Plastic Strains in Sheet-Bending," presented at the Sixth U.S. National Congress of Applied Mechanics, Harvard University, Cambridge, Mass., June 15–19, 1970.